Engineering Fracture Mechanics Vol. 43, No. 5, pp. 707–724, 1992
Printed in Great Britain.

0013-7944/92 $5.00 + 0.00

MICROMECHANICS OF ELASTIC SOLIDS WEAKENED BY A LARGE NUMBER OF CRACKS

T. C. WANG†
Institute of Mechanics, Chinese Academy of Sciences, Beijing, P.R.C.

A. EHRLACHER
C.E.R.A.M., Ecole Nationale des Ponts et Chaussées, Noisy, France

Abstract—This paper presents a micromechanics analysis of the elastic solids weakened by a large number of microcracks in a plane problem. A new cell model is proposed. Each cell is an ellipse subregion and contains a microcrack. The effective moduli and the stress intensity factors for an ellipse cell are obtained. The analytic closed formulas of concentration factor tensor for an isotropic matrix containing an anisotropic inclusion are derived. Based on a self-consistent method, the effective elastic moduli of the solids weakened by randomly oriented microcracks are obtained.

1. INTRODUCTION

THIS PAPER is concerned with micromechanics of the elastic solids weakened by a large number of microcracks. The first significant work on this subject is due to Budiansky and O'Connell [1]. Using the self-consistent method, they analysed the effect of randomly distributed penny-shaped cracks on the elastic moduli of the cracked solid. Further progress in this field has been made by Horii and Nemat-Nasser [2]. They took into account friction between opposite crack surfaces and presented an analytic closed formula for "isotropic damage" of plane cracks.

Hoenig [3] has applied the self-consistent method for aligned distributions of elliptical cracks and Grottesmann *et al.* [4] for aligned plane cracks in an orthotropic sheet. Sumarac and Krajcinovic [5] extended Horii and Nemat-Nasser's [2] work and proposed a process model through the addition of the kinetic equation. Further improvements of the self-consistent method are due to Laws and Brockenbrough [6], Salganik [7], Christensen and Lo [8], Litewka [9, 10] etc. Aboudi and Benveniste [11] have used a generalized self-consistent method for randomly oriented plane cracks. In their model, a cracked circular disk is imagined to be embedded in the effective medium. A comprehensive review on damage mechanics is given by Krajcinovic [12].

This paper presents a micromechanics analysis of the elastic solids weakened by many microcracks in the plane problem. A new cell model is proposed in this paper. The original cracked solid is divided into many cells. Each cell is an ellipse subregion and contains a microcrack in the centre. Using the complex potential method, the analytical formulas and the calculation results of the effective moduli and the stress intensity factor for the ellipse cell are obtained for different aspect ratios and different values of damage. From these results, the effective elastic moduli and the stress intensity factor for the solids weakened by a doubly periodic array of aligned microcracks are directly obtained. In order to get the effective elastic moduli of the solids weakened by random distribution of microcracks, the analytic closed formulas of concentration factor tensor for an isotropic homogeneous matrix and an anisotropic inclusion are derived. Based on the self-consistent method, the effective elastic moduli of the solids weakened by random orientation of microcracks are presented.

Finally, this study reveals that a one-parameter: crack density parameter cannot completely describe the effect of random distribution of microcracks on the elastic moduli.

Both the crack density parameter and the damage parameter, which have been introduced by Kachanov [13] and Lemaître and Chaboche [14], are important in the present study.

†Visiting Professor, E.N.P.C. January–June 1990.

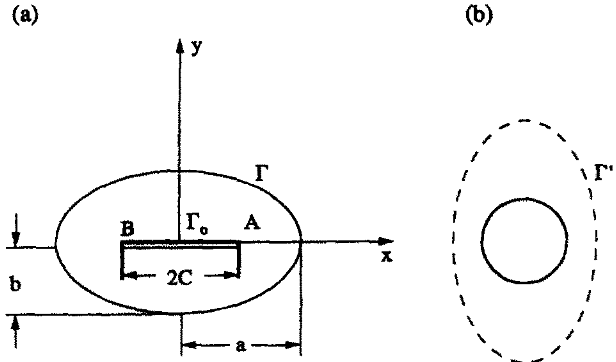

Fig. 1. An ellipse cell. (a) Physical plane. (b) Image plane.

2. CELL MODEL

In this section, we present a new cell model. The original cracked solid is divided into numerous cells. Each cell is considered to be an ellipse subregion, which contains a microcrack in the centre. In other words, each microcrack is embedded in an ellipse cell, as shown in Fig. 1.

In order to get the effective moduli of the ellipse cell, the following boundary value problem is analysed.

The equilibrium equations for the stress field are:

$$\sigma_{ij,j} = 0, \quad x \in D'; \tag{1}$$

the traction-free condition on the crack faces is:

$$\sigma_y = \tau_{xy} = 0, \quad x \in \Gamma_0; \tag{2}$$

the boundary condition on the boundary Γ is:

$$p_i = \sigma_{ij}^{(0)} n_j \quad x \in \Gamma \tag{3}$$

where $\sigma_{ij}^{(0)}$ is a uniform stress field.

According to Muskhelishvili [15], the general formulas of complex potential theory of elasticity can be expressed as:

$$\sigma_x + \sigma_y = 2[\Phi_*(Z) + \overline{\Phi_*(Z)}] \tag{4}$$

$$\sigma_y - \sigma_x + 2i\tau_{xy} = 2[\bar{Z}\Phi'_*(Z) + \Psi_*(Z)] \tag{5}$$

$$2\mu(u_x + iu_y) = \kappa\phi_*(Z) - Z\overline{\phi'_*(Z)} - \overline{\psi_*(Z)} \tag{6}$$

where $\Phi_*(Z) = \phi'_*(Z)$, $\Psi(Z) = \psi'_*(Z)$ are complex functions, holomorphic in D'. D' is the region occupied by the elastic body. Introducing the function:

$$\Omega_*(Z) = \bar{\Phi}_*(Z) + Z\bar{\Phi}'_*(Z) + \bar{\Psi}_*(Z), \tag{7}$$

we have:

$$\sigma_y - i\tau_{xy} = \Phi_*(Z) + \Omega_*(z) + (Z - \bar{Z})\overline{\Phi'_*(Z)}. \tag{8}$$

The traction-free conditions on the crack faces lead to:

$$\Phi_*^+(t) + \Omega_*^-(t) = 0, \quad t \in \Gamma_0 \tag{9a}$$

$$\Phi_*^-(t) + \Omega_*^+(t) = 0, \quad t \in \Gamma_0. \tag{9b}$$

From eq. (9), it follows that:

$$\Phi_*^{(0)}(Z) = \Phi_*(Z) - \Omega_*(Z)$$

$$\Phi_*^{(1)}(Z) = \frac{\sqrt{(Z^2 - C^2)}}{C} \cdot [\Phi_*(Z) + \Omega_*(Z)], \tag{10}$$

where $\Phi_*^{(0)}(Z)$ and $\Phi_*^{(1)}(Z)$ are holomorphic in D. Here D is the entire region inside the boundary Γ.

Equation (10) can be written as:

$$\Phi_*(Z)=\frac{1}{2}\left\{\frac{C}{\sqrt{(Z^2-C^2)}}\Phi_*^{(1)}(Z)+\Phi_*^{(0)}(Z)\right\}$$

$$\Omega_*(Z)=\frac{1}{2}\left\{\frac{C}{\sqrt{(Z^2-C^2)}}\Phi_*^{(1)}(Z)-\Phi_*^{(0)}(Z)\right\}. \tag{11}$$

Since the functions $\Phi_*^{(0)}(Z)$ and $\Phi_*^{(1)}(Z)$ are holomorphic in D, the following series expansion is available:

$$\Phi_*^{(0)}(Z)=\sum_{k=0,1}^{\infty}\alpha_k Z^k \tag{12}$$

$$\Phi_*^{(1)}(Z)=\sum_{k=0,1}^{\infty}\gamma_k Z^k. \tag{13}$$

We introduce the transformation:

$$Z=\omega(\zeta)=\frac{c}{2}\left(\zeta+\frac{1}{\zeta}\right). \tag{14}$$

The unit circle $|\zeta|=1$ in the image plane corresponds to the crack Γ_0 in the physical plane.

Substituting eq. (14) into eqs (12) and (13) we obtain:

$$\Phi(\zeta)=\Phi_*(\omega(\zeta))=\left(\frac{1}{\zeta-1}-\frac{1}{\zeta+1}\right)\gamma_0^*+\gamma_0^*+\left(\frac{1}{\zeta+1}+\frac{1}{\zeta-1}\right)\gamma_1^*+\sum_{k=-\infty}^{\infty}\beta_k^*\zeta^k \tag{15}$$

$$\Omega(\zeta)=\left(\frac{1}{\zeta-1}-\frac{1}{\zeta+1}\right)\gamma_0^*+\gamma_0^*+\left(\frac{1}{\zeta-1}+\frac{1}{\zeta+1}\right)\gamma_1^*-\sum_{k=-\infty}^{\infty}\beta_k^*\zeta^{-k}, \tag{16}$$

where γ_0^*, γ_1^* and β_k^* are unknown coefficients.

From the condition of single-valuedness of displacements (which will be proved later), we get:

$$\gamma_1^*=\tfrac{1}{2}(\beta_1^*-\beta_{-1}^*). \tag{17}$$

The remaining coefficients must be determined from the boundary condition on Γ.

We have:

$$\sigma_{\rho\rho}-i\tau_{\rho\theta}=\Phi(t)+\overline{\Phi(t)}+\mathrm{e}^{-2\alpha i}\left\{\bar{\Omega}(t)-\Phi(t)+\frac{\overline{\omega(t)}-\omega(t)}{\omega'(t)}\Phi'(t)\right\} \tag{18}$$

where $\sigma_{\rho\rho}$ and $\rho_{\rho\theta}$ are the components of stress in the curvilinear coordinate systems. Since the boundary traction on Γ is produced by the uniform stress $\sigma_{\alpha\beta}^{(0)}$, we have the following boundary condition:

$$\Phi(t)+\overline{\Phi(t)}+\mathrm{e}^{-2\alpha i}\left\{\bar{\Omega}(t)-\Phi(t)+\frac{\overline{\omega(t)}-\omega(t)}{\omega'(t)}\Phi'(t)\right\}$$
$$=\tfrac{1}{2}\{\sigma_y^{(0)}+\sigma_x^{(0)}+\mathrm{e}^{-2\alpha i}(\sigma_y^{(0)}-\sigma_x^{(0)}+2i\tau_{xy}^{(0)})\}, \tag{19}$$

where $t=\rho\,\mathrm{e}^{i\theta}$ and α is the angle between the y axis and the unit normal of Γ. We have:

$$\tan\alpha=-\frac{\mathrm{d}y}{\mathrm{d}x}=\frac{b^2x}{a^2y}=\frac{b^2\left(\rho+\frac{1}{\rho}\right)\cos\theta}{a^2\left(\rho-\frac{1}{\rho}\right)\sin\theta}. \tag{20}$$

The image of the boundary Γ is a closed curve Γ' as shown in Fig. 1b. We have the following parameter equation for the curve Γ':

$$\left[\frac{c}{2a}\left(\rho+\frac{1}{\rho}\right)\right]^2\cos^2\theta+\left[\frac{c}{2b}\left(\rho-\frac{1}{\rho}\right)\right]^2\sin^2\theta=1. \tag{21}$$

Solving this equation leads to:

$$\rho = \sqrt{[\tfrac{1}{2}(d + \sqrt{[d^2 - 4]})]} > 1. \tag{22}$$

Here:

$$d = \frac{\left[1 + 2\left(\frac{c}{2b}\right)^2 \sin^2\theta - 2\left(\frac{c}{2a}\right)^2 \cos^2\theta\right]}{\left[\left(\frac{c}{2a}\right)^2 \cos^2\theta + \left(\frac{c}{2b}\right)^2 \sin^2\theta\right]}. \tag{23}$$

Substituting eqs (15) and (16) into (19), we find:

$$\sum_{k=-\infty}^{\infty} [A_k^{(1)}(\theta)\beta_k + A_k^{(2)}(\theta)\bar{\beta}_k] + B^{(1)}(\theta)\gamma_0 + B^{(2)}(\theta)\bar{\gamma}_0 + C^{(1)}(\theta)\gamma_1 + C^{(2)}(\theta)\bar{\gamma}_1 = F(\theta), \tag{24}$$

where

$$\beta_k = \rho_0^k \beta_k^*, \quad \gamma_0 = \gamma_0^*, \quad \gamma_1 = \rho_0 \gamma_1^* \tag{25}$$

$$\rho_0 = (\rho)_{\theta=0}, \quad \sigma = e^{i\theta} \tag{26}$$

$$A_k^{(1)}(\theta) = \left(\frac{\rho}{\rho_0}\right)^k \left\{\sigma^k - e^{-2\alpha i}\left[\sigma^k + \frac{(\rho^2 - 1)(\sigma^2 - 1)}{(\rho^2\sigma^2 - 1)} k\sigma^k\right]\right\} \tag{27}$$

$$A_k^{(2)}(\theta) = \left(\frac{\rho}{\rho_0}\right)^k \left\{\sigma^{-k} - e^{-2\alpha i}\frac{\sigma^{-k}}{\rho^{2k}}\right\} \tag{28}$$

$$B^{(1)}(\theta) = \left(\frac{2}{\zeta^2 - 1} + 1\right)(1 - e^{-2\alpha i}) + e^{-2\alpha i}\frac{(\rho^2 - 1)(\sigma^2 - 1)}{(\zeta^2 - 1)}\zeta\left[\frac{1}{(\zeta - 1)^2} - \frac{1}{(\zeta + 1)^2}\right] \tag{29}$$

$$B^{(2)}(\theta) = \overline{\left(\frac{2}{\zeta^2 - 1}\right)} + 1 + e^{-2\alpha i}\left[\frac{2}{\zeta^2 - 1} + 1\right] \tag{30}$$

$$C^{(1)}(\theta) = \frac{2\zeta}{\rho_0(\zeta^2 - 1)}\left\{1 + \frac{1}{2}e^{-2\alpha i}\cdot(\rho^2 - 1)(\sigma^2 - 1)\left[\frac{1}{(\zeta - 1)^2} + \frac{1}{(\zeta + 1)^2}\right]\right\} \tag{31}$$

$$C^{(2)}(\theta) = \left\{\overline{\left(\frac{2\zeta}{(\zeta^2 - 1)}\right)} + e^{-2\alpha i}\left(\frac{2\zeta}{\zeta^2 - 1}\right)\right\}\frac{1}{\rho_0}, \quad \zeta = \rho\, e^{i\theta} \tag{32}$$

$$F(\theta) = \tfrac{1}{2}\{\sigma_y^{(0)} + \sigma_x^{(0)} + e^{-2\alpha i}(\sigma_y^{(0)} - \sigma_x^{(0)} + 2i\tau_{xy}^{(0)})\}. \tag{33}$$

Multiplying both sides of eq. (24) by $e^{im\theta}$ and integrating along Γ', we arrive at:

$$\sum_{k=-\infty}^{\infty} [A_{mk}^{(1)}\beta_k + A_{mk}^{(2)}\bar{\beta}_k] + B_m^{(1)}\gamma_0 + B_m^{(2)}\bar{\gamma}_0 + C_m^{(1)}\gamma_1 + C_m^{(2)}\bar{\gamma}_1 = F_m, \quad m = 0, \pm 1, \pm 2, \ldots, \tag{34}$$

where

$$A_{mk}^{(\alpha)} = \int_{-\pi}^{\pi} A_k^{(\alpha)}(\theta) e^{im\theta}\, d\theta$$

$$B_m^{(\alpha)} = \int_{-\pi}^{\pi} B^{(\alpha)}(\theta) e^{im\theta}\, d\theta$$

$$C_m^{(\alpha)} = \int_{-\pi}^{\pi} C^{(\alpha)}(\theta) e^{im\theta}\, d\theta \quad \alpha = 1, 2. \tag{35}$$

The integrals in eq. (35) were carried out by numerical integration. From 400 up to 2000 integration points were used in the numerical calculation. Truncating the series and solving eq. (34), one finds the coefficients β_k, γ_0 and γ_1.

The displacement field can be expressed as:

$$2\mu(u_x + iu_y) = \kappa\phi_*(Z) - W_*(\bar{Z}) - (Z - \bar{Z})\overline{\Phi_*(Z)}, \tag{36}$$

where

$$W_*(Z) = \int \Omega_*(Z)\,\mathrm{d}Z = Z\bar{\Phi}_*(Z) + \bar{\Psi}_*(Z).$$

Using eqs (14) and (15), it follows that:

$$\phi(\zeta) = \frac{C}{2}\left\{ \sum_{\substack{n=\infty \\ m\neq -1}}^{\infty} \frac{\beta_m^* \zeta^{m+1}}{(m+1)} + \sum_{\substack{m=-\infty \\ m\neq -1}}^{\infty} \frac{\beta_{-m}^*}{(m+1)} \zeta^{-m-1} + [2\gamma_1^* - (\beta_1^* - \beta_{-1}^*)] \ln \zeta - \frac{2\gamma_0^*}{\zeta} + \gamma_0^*\left(\zeta + \frac{1}{\zeta}\right)\right\} \tag{37}$$

$$W(\zeta) = W_*(\omega(\zeta)) = \frac{C}{2}\left\{ - \sum_{\substack{m=-\infty \\ m\neq -1}}^{\infty} \frac{(\beta_{-m}^* \zeta^{m+1} + \beta_m^* \zeta^{-m-1})}{(m+1)} + [2\gamma_1^* - (\beta_1^* - \beta_{-1}^*)] \ln \zeta - \frac{2\gamma_0^*}{\zeta} + \gamma_0^*\left(\zeta + \frac{1}{\zeta}\right)\right\}. \tag{38}$$

The condition of single-valuedness of displacements leads to:

$$\gamma_1^* = \tfrac{1}{2}(\beta_1^* - \beta_{-1}^*). \tag{39}$$

The overall strain is:

$$\hat{\epsilon}_{\alpha\beta} = \frac{1}{\pi ab} \iint_D \epsilon_{\alpha\beta}\,\mathrm{d}x\,\mathrm{d}y = \frac{1}{\pi ab} \int_\Gamma (u_\alpha n_\beta + u_\beta n_\alpha)\,\mathrm{d}s, \tag{40}$$

where n_α is the direction cosine of the unit normal of the boundary Γ. We have:

$$n_x\,\mathrm{d}s = \mathrm{d}y = \frac{C}{2}\left\{\left(\rho - \frac{1}{\rho}\right)\cos\theta + \left(1 + \frac{1}{\rho^2}\right)\frac{\mathrm{d}\rho}{\mathrm{d}\theta}\sin\theta\right\} \tag{41}$$

$$n_y\,\mathrm{d}s = -\mathrm{d}x = \frac{C}{2}\left\{\left(\rho + \frac{1}{\rho}\right)\sin\theta - \left(1 - \frac{1}{\rho^2}\right)\frac{\mathrm{d}\rho}{\mathrm{d}\theta}\cos\theta\right\}\mathrm{d}\theta. \tag{42}$$

From eq. (21), it follows that:

$$\frac{\mathrm{d}\rho}{\mathrm{d}\theta} = \frac{\rho\left\{\left(\frac{C}{2a}\right)^2\left(\rho + \frac{1}{\rho}\right)^2 - \left(\frac{C}{2b}\right)^2\left(\rho - \frac{1}{\rho}\right)^2\right\}\sin 2\theta}{2\left(\rho^2 - \frac{1}{\rho^2}\right)\left[\left(\frac{C}{2a}\right)\cos^2\theta + \left(\frac{C}{2b}\right)^2\sin^2\theta\right]}. \tag{43}$$

We introduce the following integrals:

$$P_x = \int_\Gamma (u_x + iu_y) n_x\,\mathrm{d}s$$

$$P_y = \int_\Gamma (u_x + iu_y) n_y\,\mathrm{d}s. \tag{44}$$

Substituting eq. (44) into eq. (40), we obtain:

$$\hat{\epsilon}_x = \mathrm{Re}\{P_x\}/\pi ab$$

$$\hat{\epsilon}_y = \mathrm{Im}\{P_y\}/\pi ab$$

$$\hat{\epsilon}_{xy} = \tfrac{1}{2}\{\mathrm{Im}\{P_x\} + \mathrm{Re}\{P_y\}\}/\pi ab. \tag{45}$$

Following Horii and Nemat-Nasser [2], we introduce the overall stress and strain vectors:

$$\hat{\boldsymbol{\sigma}} = [\sigma_x^{(0)}\ \sigma_y^{(0)}\ \tau_{xy}^{(0)}]^T \tag{46}$$

$$\hat{\boldsymbol{\epsilon}} = [\hat{\epsilon}_x\ \hat{\epsilon}_y\ \hat{\epsilon}_{xy}]^T. \tag{47}$$

The strain vector $\hat{\boldsymbol{\varepsilon}}$ can be represented as:

$$\hat{\boldsymbol{\varepsilon}} = \mathbb{M}\hat{\boldsymbol{\sigma}}, \tag{48}$$

where the matrix $\mathbb{M}$ is the effective elastic compliance tensor. Let $\sigma_x^{(0)} = 1$, $\sigma_y^{(0)} = \tau_{xy}^{(0)} = 0$; one can get:

$$\hat{\boldsymbol{\varepsilon}} = [M_{11} \;\; M_{21} \;\; M_{31}]^T.$$

Similarly we can find all components of M_{ij}.

The stress intensity factors at the crack tip A take the forms:

$$K_{\mathrm{I}} = \sigma_y^{(0)}\sqrt{(\pi C)}\,f\left(\frac{b}{a}, \frac{c}{a}\right)$$

$$K_{\mathrm{II}} = \tau_{xy}^{(0)}\sqrt{(\pi C)}\,g\left(\frac{b}{a}, \frac{c}{a}\right). \tag{49}$$

One can easily find that both crack tips A and B have the same stress intensity factors.

The calculation was performed for the case of plane strain with $\nu = 0.3$ (ν is the Poisson's ratio of the virgin material).

The compliance tensor of the undamaged material in plane strain is:

$$\mathbb{M} = \frac{1}{2\mu}\begin{bmatrix} 1-\nu & -\nu & 0 \\ -\nu & 1-\nu & 0 \\ 0 & 0 & 1 \end{bmatrix}. \tag{50}$$

The calculations show that the crack has no effect on the components M_{11}, M_{12}, M_{13}; M_{21}, M_{23}; M_{31}, M_{32}. Only the compliances M_{22} and M_{33} are changed.

Hence we just discuss the values of M_{22} and M_{33}. It is convenient to introduce the nondimensional compliance tensor:

$$\mathbf{m} = 2\mu \cdot \mathbb{M}. \tag{51}$$

The relations between m_{22} and the damage parameter c/a for different aspect ratios b/a are shown in Fig. 2.

The variations of m_{33} with the damage parameter c/a are plotted in Fig. 3 for different aspect ratios b/a. Figure 4 shows the compliances m_{21}, m_{22} and m_{23} for the case of $b/a = 0.5$. We observe that the smaller is the aspect ratio b/a, the greater are the compliances. On the other hand,

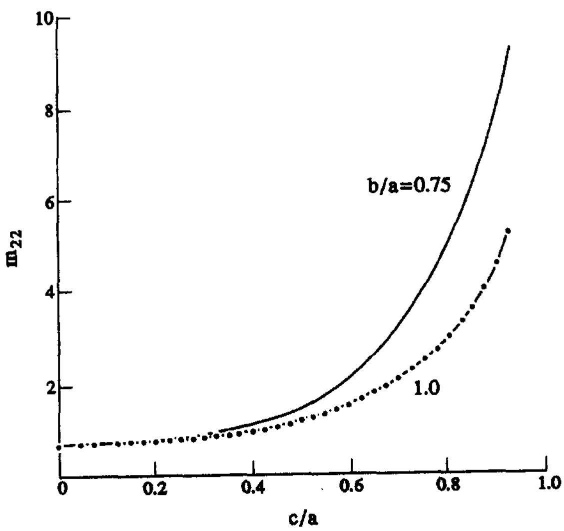

Fig. 2. Nondimensional effective compliance m_{22} of the ellipse cell versus damage parameter c/a for aspect ratio $b/a = 1$ and 0.75.

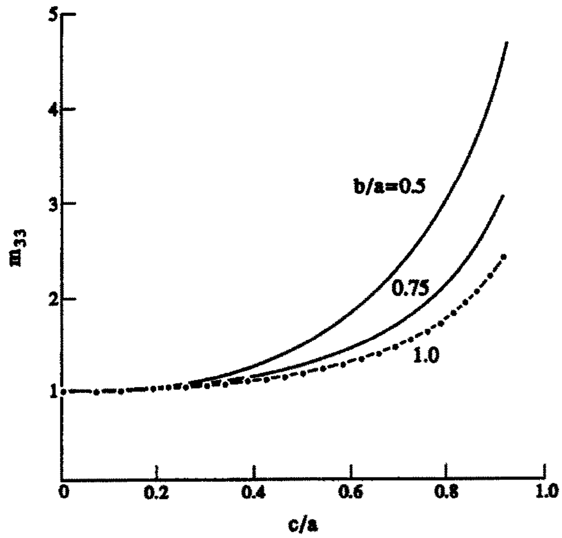

Fig. 3. Nondimensional effective compliance m_{33} of the ellipse cell versus the damage parameter c/a for aspect ratio $b/a = 1$, 0.75 and 0.5.

the compliance m_{22} increases faster than that of m_{33} when the damage parameter c/a increases. The parameters f and g versus c/a are plotted in Figs 5 and 6.

3. PERIODIC ARRAY OF ALIGNED CRACKS

The above results can be directly applied to the case of elastic solids weakened by a double periodic array of aligned cracks. As shown in Fig. 7, H_1 and H_2 represent the distances between adjacent cracks in the x and y directions respectively.

Of course, the effective elastic modulus of the cracked solid is exactly equal to the effective elastic modulus of the rectangular cell, as shown in Fig. 7.

The effective elastic modulus of the rectangular cell is considered to be approximately equal to the effective elastic modulus of an elliptic cell if we choose the major semi-axis $a = H_1/2$ and the minor semi-axis $b = 2H_2/\pi$. This means that both cells have the same area. Similarly, using the elliptic cell, the stress intensity factors of the original cracked solid can be approximately estimated.

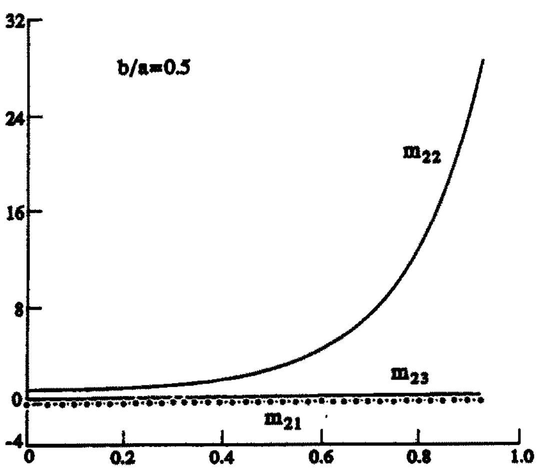

Fig. 4. Normalized compliances m_{21}, m_{22} and m_{23} for $b/a = 0.5$.

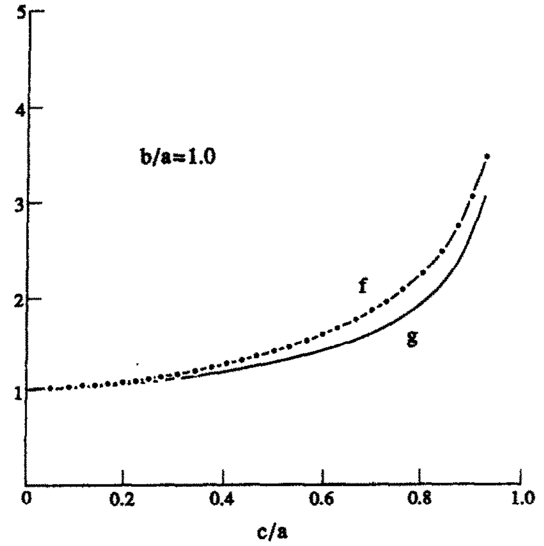

Fig. 5. Stress intensity factor parameters f and g of the ellipse cell for $b/a = 1.0$.

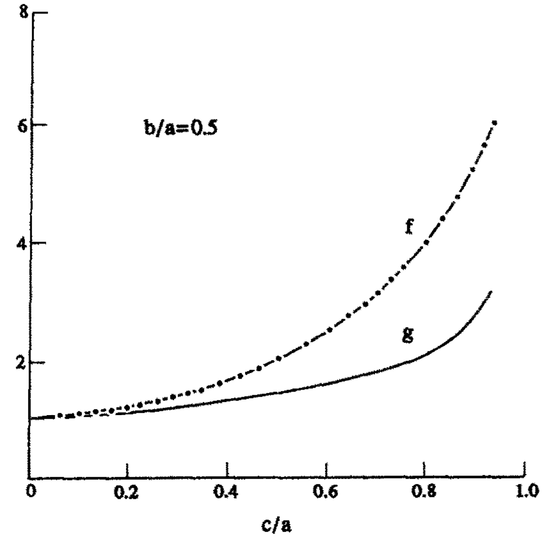

Fig. 6. Stress intensity factor parameters f and g of the ellipse cell for $b/a = 0.5$.

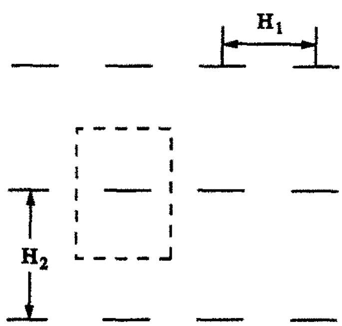

Fig. 7. An elastic solid weakened by a double periodic array of aligned cracks.

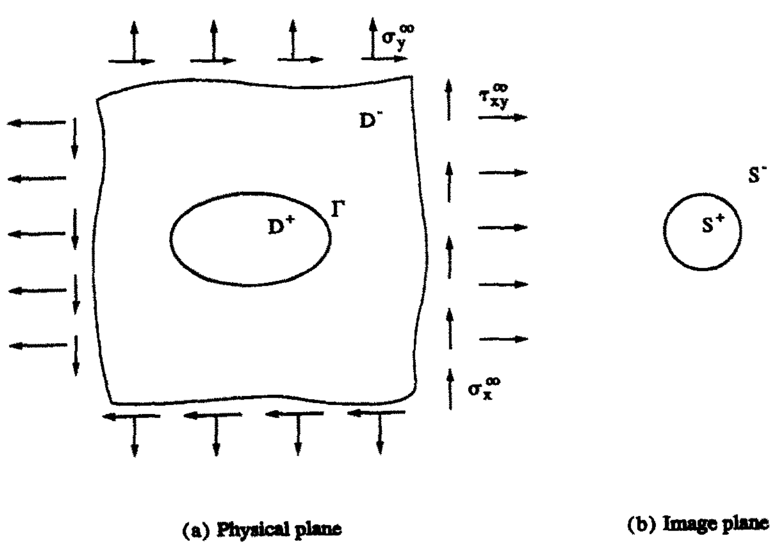

Fig. 8. An anisotropic inclusion embedded in an isotropic matrix.

4. CONCENTRATION FACTOR TENSOR

Eshelby [16] has provided a well known solution for the general ellipsoidal inclusion. He pointed out that the stress and strain fields in the ellipsoidal inclusion embedded in a homogeneous elastic matrix, subjected to uniform stresses at infinity, are uniform as well.

Hence we have:

$$\mathfrak{E} = \mathbb{A}\varepsilon^{\infty}. \tag{52}$$

The tensor $\mathbb{A}$ defined in eq. (52) is called the concentration factor tensor in the literature. Generally speaking, the calculation of tensor $\mathbb{A}$ involves nontrivial numerical quadratures of complicated integrals.

In this section, the analytic closed formulas of the concentration factor tensor for an isotropic homogeneous matrix and an anisotropic inclusion are derived in the two-dimensional plane problem.

As shown in Fig. 8, an anisotropic ellipse inclusion is embedded in an isotropic homogeneous matrix.

We use the following transformation:

$$Z = \omega(\zeta) = R\left(\zeta + \frac{m}{\zeta}\right). \tag{53}$$

The region D^-, which is occupied by the isotropic matrix, will transform onto the region $|\zeta| \geqslant 1$. The unit circle $|\zeta| = 1$ corresponds to the ellipse Γ with centre at the origin and semi-axes:

$$a = R(1+m), \quad b = R(1-m). \tag{54}$$

Let $\sigma_{\alpha\beta}^{(0)}$ denote the uniform stress field inside the inclusion. The matrix can be considered as an infinite plate with an elliptic hole which is subject to traction obtained by uniform stress field $\sigma_{\alpha\beta}^{(0)}$.

On the unit circle, we have the following boundary condition:

$$\Phi^-(\sigma) + \overline{\Phi^-(\sigma)} + \frac{(\sigma^2 - m)}{(m\sigma^2 - 1)}\left\{\frac{\overline{\omega(\sigma)}}{\omega'(\sigma)}\Phi'^-(\sigma) + \Psi^-(\sigma)\right\}$$
$$= \frac{1}{2}\left\{\sigma_y^{(0)} + \sigma_x^{(0)} + \frac{(\sigma^2 - m)}{(m\sigma^2 - 1)}(\sigma_y^{(0)} - \sigma_x^{(0)} + 2i\tau_{xy}^{(0)})\right\} \tag{55}$$

where $\sigma = e^{i\theta}$.

We introduce the following function:

$$\Omega(z) = \begin{cases} \bar{\Phi}\left(\dfrac{1}{\zeta}\right), & \zeta \in S^+ \\ -\left[\Phi(\zeta) + \dfrac{(\zeta^2 - m)}{(m\zeta^2 - 1)}\left(\dfrac{\zeta(m\zeta^2 + 1)}{(\zeta^2 - m)}\Phi'(\zeta) + \Psi(\zeta)\right)\right], & \zeta \in S^-. \end{cases} \tag{56}$$

The function $\Omega(\zeta)$ is holomorphic in both regions S^+ and S^-. The boundary condition (55) can be expressed as:

$$\Omega^+(\sigma) - \Omega^-(\sigma) = \frac{1}{2}\left\{\sigma_y^{(0)} + \sigma_x^{(0)} + \frac{(\sigma^2 - m)}{(m\sigma^2 - 1)}(\sigma_y^{(0)} - \sigma_x^{(0)} + 2\tau_{xy}^{(0)}i)\right\}. \tag{57}$$

The special solution for eq. (57) takes the form:

$$\Omega_0(\zeta) = \begin{cases} 0, & \zeta \in S^{-1} \\ \dfrac{1}{2}\left\{(\sigma_y^{(0)} + \sigma_x^{(0)}) + \dfrac{(\zeta^2 - m)}{(m\zeta^2 - 1)}(\sigma_y^{(0)} - \sigma_x^{(0)} + 2\tau_{xy}^{(0)}i)\right\}, & \zeta \in S^+. \end{cases} \tag{58}$$

Thus the homogeneous solution $\Omega_h(\zeta)$ of eq. (57) must be holomorphic in the whole ζ plane except possible poles $\zeta = \pm R_0 (R_0 = 1/\sqrt{(m)})$ and the point $\zeta = \infty$.

Near the point $\zeta = \infty$, we have:

$$\Omega_h(\zeta) = \gamma - R_0^2\gamma' + 0\left(\frac{1}{\zeta}\right), \quad R_0 = \frac{1}{\sqrt{(m)}}. \tag{59}$$

Near the pole $\zeta = R_0$, we find:

$$\Omega_h(\zeta) = \frac{A_1}{(\zeta - R_0)} + O(1) \tag{60}$$

where

$$A_1 = -\left\{R_0^2\Phi'(R_0) + \frac{R_0\left(R_0^2 - \frac{1}{R_0^2}\right)}{2}\Psi(R_0)\right\}.$$

Near the pole $\zeta = -R_0$, we have:

$$\Omega_h(\zeta) = \frac{A_2}{(\zeta + R_0)} + O(1)$$

$$A_2 = R_0^2\Phi'(-R_0) + \frac{R_0\left(R_0^2 - \frac{1}{R_0^2}\right)}{2}\Psi(-R_0). \tag{61}$$

From eqs (59)–(61), we arrive at:

$$\Omega_h(\zeta) = -\gamma - R_0^2\gamma' + \frac{A_1}{(\zeta - R_0)} + \frac{A_2}{(\zeta + R_0)}. \tag{62}$$

Thus we obtain:

$$\Omega(\zeta) = \Omega_0(\zeta) + \Omega_h(\zeta) \tag{63}$$

$$\Phi(\zeta) = \bar{\Omega}\left(\frac{1}{\zeta}\right) = -\bar{\gamma} - R_0^2\gamma' + \frac{\bar{A}_1\zeta}{(1 - R_0\zeta)} + \frac{\bar{A}_2\zeta}{(1 + R_0\zeta)}, \quad \zeta \in S^-. \tag{64}$$

For large ζ we have:

$$\Phi(\zeta) = \gamma + O\left(\frac{1}{\zeta^2}\right). \tag{65}$$

Comparison of eqs (64) and (65) gives:

$$\begin{aligned}(\bar{A}_2 - \bar{A}_1)/R_0 &= \gamma + \bar{\gamma} + R_0^2\bar{\gamma}' - \bar{\Omega}_0(0)\\ \bar{A}_1 + \bar{A}_2 &= 0.\end{aligned} \tag{66}$$

The solution of eq. (66) is:

$$\begin{aligned}\bar{A}_1 &= -\bar{A}_2\\ \bar{A}_2 &= \frac{R_0}{2}A_0, \quad A_0 = \gamma + \bar{\gamma} + R_0^2\bar{\gamma}' - \bar{\Omega}_0(0).\end{aligned} \tag{67}$$

From eq. (56) one finds:

$$\Psi(\zeta) = -\frac{(\zeta^2 - R_0^2)}{(R_0^2\zeta^2 - 1)}[\Phi(\zeta) + \Omega(\zeta)] - \frac{\zeta(\zeta^2 + R_0^2)}{(R_0^2\zeta^2 - 1)}\Phi'(\zeta), \quad \zeta \in S^-. \tag{68}$$

Comparing eq. (68) with eq. (125.8) of Muskhelishvili [15], one concludes that the function $\Omega(\zeta)$ defined here is equal to the function $\bar{\phi}(1/\zeta)$ introduced by Muskhelishvili [15]. Hence we can directly use the formulas given by Muskhelishvili [15].

After some manipulations, it follows that:

$$\Phi(\zeta)=\begin{cases}\dfrac{A_0}{(R_0^2\zeta^2-1)}+\bar{\Omega}_0\left(\dfrac{1}{\zeta}\right)-\bar{\Omega}_0(0)+\gamma, & \zeta\in S^-\\[2ex] \dfrac{A_0}{(R_0^2\zeta^2-1)}+\gamma-\bar{\Omega}_0(0), & \zeta\in S^+.\end{cases}\tag{69}$$

Noting that:

$$\bar{\Omega}_0(0)=\frac{1}{2}\left\{\sigma_x^{(0)}+\sigma_y^{(0)}+\frac{1}{R_0^2}(\sigma_y^{(0)}-\sigma_x^{(0)}-2\tau_{xy}^{(0)}i)\right\}\tag{70}$$

$$\gamma=\tfrac{1}{4}(N_1+N_2)=\tfrac{1}{4}(\sigma_x^\infty+\sigma_y^\infty)\tag{71}$$

$$\gamma'=\tfrac{1}{2}(N_2-N_1)e^{-2\alpha i}=\tfrac{1}{2}(\sigma_y^\infty-\sigma_x^\infty+2i\tau_{xy}^\infty)\tag{72}$$

where $\sigma_{\alpha\beta}^\infty$ is the value of the stress component at infinity and α the angle between principal stress N_1 and the OX axis.

Equation (69) can be represented as:

$$\Phi(\zeta)=\begin{cases}\dfrac{A_0^*}{(R_0^2\zeta^2-1)}+\gamma, & \zeta\in S^-\\[2ex] \dfrac{A_0}{(R_0^2\zeta^2-1)}+\gamma-\bar{\Omega}_0(0), & \zeta\in S^+\end{cases}\tag{73}$$

where

$$A_0^*=\tfrac{1}{2}\{\sigma_y^\infty+\sigma_x^\infty+R_0^2(\sigma_y^\infty-\sigma_x^\infty-2\tau_{xy}^\infty i)\}-\tfrac{1}{2}\{\sigma_y^{(0)}+\sigma_x^{(0)}+R_0^2(\sigma_y^{(0)}-\sigma_x^{(0)}-2\tau_{xy}^{(0)}i)\}.\tag{74}$$

Using eq. (73), one finds:

$$\phi(\zeta)=\begin{cases}-Rm\dfrac{A_0^*}{\zeta}+\gamma\omega(\zeta), & \zeta\in S^-\\[2ex] -Rm\dfrac{A_0^*}{\zeta}+(\gamma-\bar{\Omega}_0(0))\omega(\zeta), & \zeta\in S^+.\end{cases}\tag{75}$$

The displacement components u_x and u_y on the unit circle $|\zeta|=1$ will be:

$$2\mu(u_x+iu_y)=\kappa\phi(\zeta)+\phi\left(\frac{1}{\bar{\zeta}}\right)-\left(\omega(\zeta)-\omega\left(\frac{1}{\bar{\zeta}}\right)\right)\overline{\Phi(\zeta)}.\tag{76}$$

Substituting eq. (75) into eq. (76), we obtain:

$$2\mu(u_x+iu_y)=R\left(q_1\zeta+q_{-1}\frac{1}{\zeta}\right),\quad \text{on } |\zeta|=1.\tag{77}$$

Here:

$$q_1=\kappa\gamma+\gamma-\bar{\Omega}_0(0)\tag{78}$$

$$q_{-1}=m\kappa(\gamma-A_0^*)-m\bar{\gamma}-\bar{\gamma}.\tag{79}$$

Denoting:

$$\begin{aligned}q_1&=C_{11}+iC_{12}\\ q_{-1}&=C_{21}+iC_{22},\end{aligned}\tag{80}$$

one finds:

$$C_{11}=\kappa\gamma+\left\{\frac{1}{4}(\sigma_x^\infty+\sigma_y^\infty)-\frac{1}{2}(\sigma_x^{(0)}+\sigma_y^{(0)})-\frac{m}{2}(\sigma_y^{(0)}-\sigma_x^{(0)})\right\}\tag{81}$$

$$C_{12}=\tau_{xy}^{(0)}\tag{82}$$

$$C_{21} = \kappa\left\{\frac{m}{2}(\sigma_x^{(0)} + \sigma_y^{(0)}) - \frac{1}{2}(\sigma_y^{(0)} - \sigma_x^{(0)})\right\} - \frac{m}{2}(\sigma_x^{\infty} + \sigma_y^{\infty}) - \frac{1}{2}(\sigma_y^{\infty} - \sigma_x^{\infty}) - m\gamma - \frac{1}{2}(\sigma_y^{\infty} - \sigma_x^{\infty}) \quad (83)$$

$$C_{22} = \kappa(\tau_{xy}^{\infty} - \tau_{xy}^{(0)}) + \tau_{xy}^{\infty}. \quad (84)$$

On the ellipse boundary, we have $\zeta = e^{i\theta}$.

From eqs (77)–(80), it follows that:

$$2\mu u_x = R\{(C_{11} + C_{12})\cos\theta + (C_{22} - C_{12})\sin\theta\} \quad (85)$$

$$2\mu u_y = R\{(C_{11} - C_{21})\sin\theta + (C_{22} + C_{12})\cos\theta\}. \quad (86)$$

On the other hand, the displacement components u_x and u_y can be expressed as:

$$u_\alpha = \epsilon_{\alpha\beta}x_\beta + \omega_{\alpha\beta}x_\beta. \quad (87)$$

Here, $\epsilon_{\alpha\beta}$ is the uniform strain inside the ellipse inclusion and $\omega_{\alpha\beta}$ is the rigid rotation of the ellipse inclusion. Keeping in mind that $\omega_{\alpha\beta}$ is an antisymmetric tensor and denoting $\omega_{21} = \omega$, eq. (87) can be rewritten as:

$$u_x = \epsilon_{11}x_1 + \epsilon_{12}x_2 - \omega x_2 = \epsilon_{11}a\cos\theta + (\epsilon_{12} - \omega)b\sin\theta, \quad (88)$$

$$u_y = \epsilon_{21}c_1 + \epsilon_{22}x_2 + \omega x_1 = (\epsilon_{21} + \omega)a\cos\theta + \epsilon_{22}b\sin\theta. \quad (89)$$

The constitutive relation of the inclusion gives:

$$\begin{aligned}
\epsilon_{11} &= M_{11}\sigma_x^{(0)} + M_{12}\sigma_y^{(0)} + M_{13}\tau_{xy}^{(0)} \\
\epsilon_{22} &= M_{21}\sigma_x^{(0)} + M_{22}\sigma_y^{(0)} + M_{23}\tau_{xy}^{(0)} \\
\epsilon_{12} &= M_{31}\sigma_x^{(0)} + M_{31}\sigma_y^{(0)} + M_{33}\tau_{xy}^{(0)}
\end{aligned} \quad (90)$$

where $\mathbb{M}$ is the compliance tensor of the inclusion.

Comparing eqs (85), (86) and (88), (89), we arrive at:

$$\begin{aligned}
C_{11} + C_{21} &= 2\mu\frac{a}{R}\epsilon_{11} \\
C_{22} - C_{12} &= 2\mu\frac{b}{R}(\epsilon_{12} - \omega) \\
C_{22} + C_{12} &= 2\mu\frac{a}{R}(\epsilon_{21} + \omega) \\
C_{11} - C_{21} &= 2\mu\frac{b}{R}\epsilon_{22}.
\end{aligned} \quad (91)$$

Eliminating ω from eq. (91), it follows that:

$$\begin{aligned}
C_{11} + C_{21} &= \frac{2\mu a}{R}\epsilon_{11} \\
C_{11} - C_{21} &= \frac{2\mu b}{R}\epsilon_{22} \\
\frac{a}{R}(C_{22} - C_{12}) + \frac{b}{R}(C_{22} + C_{12}) &= 4\mu\frac{ab}{R^2}\epsilon_{12}.
\end{aligned} \quad (92)$$

We introduce stress vectors $\boldsymbol{\sigma}^{(0)}$ and $\boldsymbol{\sigma}^{\infty}$:

$$\boldsymbol{\sigma}^{(0)} = [\sigma_x^{(0)}\ \sigma_y^{(0)}\ \tau_{xy}^{(0)}]^T \quad (93)$$

$$\boldsymbol{\sigma}^{\infty} = [\sigma_x^{\infty}\ \sigma_y^{\infty}\ \tau_{xy}^{\infty}]^T. \quad (94)$$

Equation (92) can be represented as:

$$(\mathbb{T}\mathbb{M} - \mathbb{P})\boldsymbol{\sigma}^{(0)} = \mathbb{H}\boldsymbol{\sigma}^{\infty}, \quad (95)$$

where the matrices $\mathbb{T}$, $\mathbb{H}$, and $\mathbb{P}$ are:

$$\mathbb{T} = \mathrm{diag}\left[\frac{a}{R}\frac{b}{R}\frac{2ab}{R^2}\right] \tag{96}$$

$$\mathbb{H} = \frac{1}{2\mu}\begin{bmatrix} \frac{(\kappa+1)}{4}(3-m) & \frac{(\kappa+1)}{4}(1+m) & 0 \\ \frac{(\kappa+1)(1-m)}{4} & \frac{(\kappa+1)(3-m)}{4} & 0 \\ 0 & 0 & 2(\kappa+1) \end{bmatrix} \tag{97}$$

$$\mathbb{P} = \frac{1}{2\mu}\begin{bmatrix} \frac{(\kappa+1)(1-m)}{2} & \frac{(\kappa-1)(1+m)}{2} & 0 \\ \frac{(\kappa-1)(1-m)}{2} & \frac{(\kappa+1)(1+m)}{2} & 0 \\ 0 & 0 & -2(\kappa+m^2) \end{bmatrix}. \tag{98}$$

From eq. (95) one finds

$$\boldsymbol{\sigma}^{(0)} = (\mathbb{T}\mathbb{M} - \mathbb{P})^{-1}\mathbb{H}\boldsymbol{\sigma}^{\infty} \tag{99}$$

$$\boldsymbol{\varepsilon}^{(0)} = \mathbb{M}\boldsymbol{\sigma}^{(0)} = \mathbb{M}(\mathbb{T}\mathbb{M} - \mathbb{P})^{-1}\mathbb{H}\mathscr{L}\boldsymbol{\varepsilon}^{\infty}. \tag{100}$$

Here, $\mathscr{L}$ is the elastic modulus tensor of the matrix.

Thus we obtain the concentration factor tensor $\mathbb{A}$:

$$\mathbb{A} = \mathbb{M}(\mathbb{T}\mathbb{M} - \mathbb{P})^{-1}\mathbb{H}\mathscr{L}. \tag{101}$$

All the above formulas are derived in the local coordinate system.

5. EFFECTIVE ELASTIC MODULI IN THE CASE OF A RANDOM DISTRIBUTION OF CRACKS

Now we consider the elastic solids weakened by a random distribution of microcracks. The orientations, locations and sizes of the microcracks are supposed to be sufficiently random and uncorrelated but the aspect ratio a/b of the minor semi-axis to the major semi-axis and the damage parameter c/a are the same for all ellipse cells.

As pointed out by Horii and Nemat-Nasser [2], from the local coordinate system to the global coordinate system, the stress and strain vectors obey the following transformation:

$$\boldsymbol{\varepsilon}^* = \mathbb{Q}\boldsymbol{\varepsilon}, \quad \boldsymbol{\sigma}^* = \mathbb{Q}\boldsymbol{\sigma} \tag{102}$$

where $\boldsymbol{\varepsilon}^*$ and $\boldsymbol{\sigma}$ are the strain and stress vectors in the local coordinate system, and $\mathbb{Q}$ is the transform matrix:

$$\mathbb{Q} = \begin{bmatrix} \cos^2\theta & \sin^2\theta & \sin^2\theta \\ \sin^2\theta & \cos^2\theta & -\sin^2\theta \\ -\frac{1}{2}\sin^2\theta & \frac{1}{2}\sin^2\theta & \cos^2\theta \end{bmatrix}. \tag{103}$$

For the elastic compliance tensor and the concentration factor tensor, we have:

$$\mathbb{M} = \mathbb{Q}^{-1}\mathbb{M}^*\mathbb{Q}, \tag{104}$$

$$\mathbb{A} = \mathbb{Q}^{-1}\mathbb{A}^*\mathbb{Q}. \tag{105}$$

The overall strain $\mathfrak{E}^{\infty}$ of the cracked solid should be equal to:

$$\mathfrak{E}^{\infty} = \frac{1}{V}\sum_{k=1}^{N} \mathfrak{E}_k^{(0)} V_k, \tag{106}$$

where the summation is extended over all ellipse cells, V is the volume of the cracked solid and V_k is the volume of the kth ellipse cell.

On the other hand, we have:

$$\sigma_k^{(0)} = \mathbb{L}_k \mathfrak{E}_k^{(0)} = \mathbb{L}_k \mathbb{A}_k \mathfrak{E}^{\infty}. \tag{107}$$

The overall stress vector of the cracked solid is the volume average of the stress of the constituent phase:

$$\sigma^{\infty} = \sum_{k=1}^{N} \sigma_k^{(0)} V_k / V. \tag{108}$$

Substituting eq. (107) into eq. (108), one finds:

$$\sigma^{\infty} = \sum_{k=1}^{N} (\mathbb{Q}^{-1}\mathbb{L}\mathbb{A}\mathbb{Q})_k \mathfrak{E}^{\infty} \frac{V_k}{V}. \tag{109}$$

On the other hand, we have:

$$\sigma^{\infty} = \mathscr{L}\mathfrak{E}^{\infty}. \tag{110}$$

Comparison of eqs (109) and (110) leads to:

$$\mathscr{L} = \sum_{k=1}^{N} (\mathbb{Q}^{-1}\mathbb{L}\mathbb{A}\mathbb{Q})_k \frac{V_k}{V}. \tag{111}$$

Using eqs (104) and (105), we arrive at:

$$\mathscr{L} = \sum_{k=1}^{N} (\mathbb{Q}^{-1}\mathbb{L}^*\mathbb{A}^*\mathbb{Q})_k \frac{V_k}{V}, \tag{112}$$

where the matrix $\mathbb{L}^*$ is the effective elastic moduli tensor of the ellipse cell and $\mathbb{A}^*$ is the concentration factor tensor. Both $\mathbb{L}^*$ and $\mathbb{A}^*$ are in local coordinates.

The orientation angle θ is considered to be varied in $(-\pi, \pi)$. Due to symmetry, we only consider $\theta \in (0, \pi)$. Choose $(N+1)$ integration points.

$$\theta_k = (k-1)\pi/N, \quad k = 1, 2, \ldots, N+1.$$

In our calculation, N varies from 200 to 2000. We find $N = 200$ gives the results with four digits of accuracy. Hence most calculations were carried out with $N = 200$.

Because the matrix $\mathscr{L}^*$ is related to the unknown matrix $\mathscr{L}$, hence eq. (112) needs to be solved by an iteration method. The matrix $\mathscr{L}$ is considered to be isotropic due to random distribution of cracks. We have:

$$\mathscr{L} = 2\mu \begin{bmatrix} \dfrac{\kappa+1}{2(\kappa-1)} & \dfrac{3-\kappa}{2(\kappa-1)} & 0 \\ \dfrac{3-\kappa}{2(\kappa-1)} & \dfrac{\kappa+1}{2(\kappa-1)} & 0 \\ 0 & 0 & 1 \end{bmatrix} \tag{113}$$

where μ is the effective shear modulus of the cracked solid and $\kappa = 3 - 4\nu$ for plane strain, $\kappa = (3-\nu)/(1+\nu)$ for plane stress; ν is the effective Poisson's ratio.

The calculation was performed for plane strain with the Poisson's ratio $\nu_0 = 0.3$ of the virgin material. The calculation results are shown in Figs 9 and 10. Figure 9 shows the normalized effective shear modulus μ, Young's modulus E, bulk modulus K and Poisson's ratio ν for the case $a/b = 1$. Here α is the crack density parameter:

$$\alpha = \frac{C^2}{ab}. \tag{114}$$

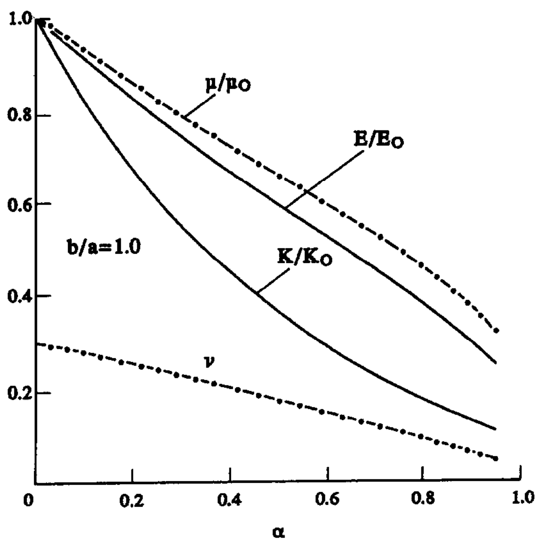

Fig. 9. Normalized effective moduli and Poisson's ratio versus crack density parameter for $b/a = 1$.

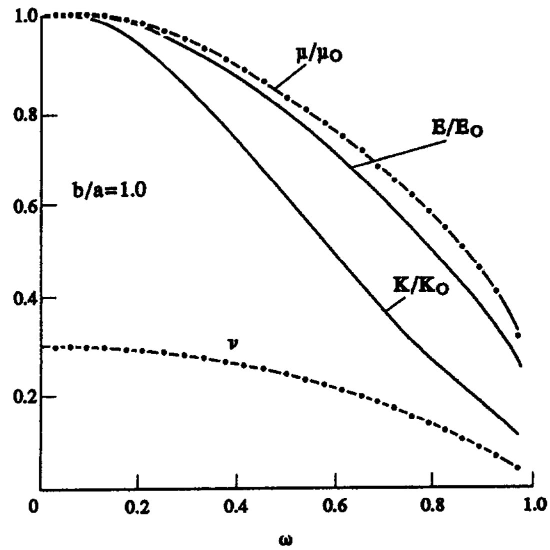

Fig. 10. Normalized effective moduli and Poisson's ratio versus damage parameter for $b/a = 1$.

μ_0, E_0 and K_0 are the elastic moduli of the virgin material. The same nondimensional variables μ, E, K and ν versus damage parameter $\omega(\omega = c/a)$ are plotted in Fig. 10.

It is worth noting that the crack density parameter α has a maximum value $\alpha_{max} = 1$. When α approaches α_{max}, the damage parameter ω approaches one, then all effective moduli seem to approach zero. This tendency is clearer in Fig. 10, especially for Young's modulus E and bulk modulus K. The effective Poisson's ratio ν shows the same behaviour.

Figure 11 shows the variations of μ/μ_0, E/E_0, K/K_0 and ν with the crack density parameter α for the case of $b/a = 0.5$. The relations between these variables and the damage parameter ω are plotted in Fig. 12.

For the case of $b/a = 0.5$, the maximum value of α is 2. When $\omega \to 1$ all effective moduli seem to approach zero. The calculation is carried out for $\omega \leqslant 0.9$. When $\omega > 0.9$, the accuracy of the calculation results is not good enough.

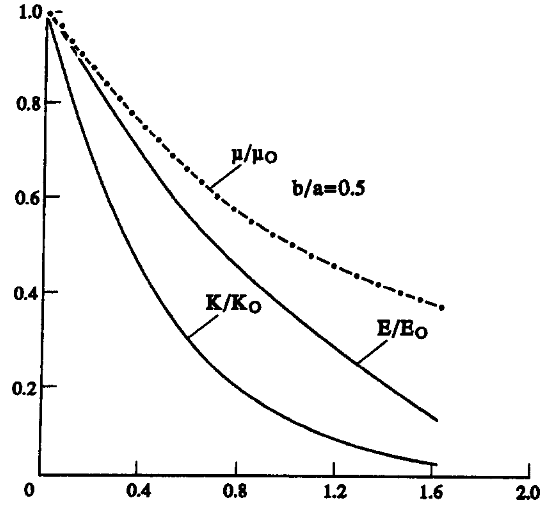

Fig. 11. Relations between effective moduli, Poisson's ratio and crack density parameter for $b/a = 0.5$.

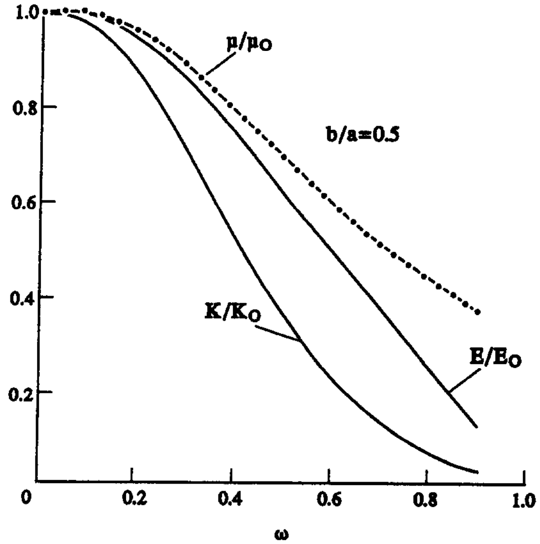

Fig. 12. Variations of effective moduli and Poisson's ratio with damage parameter for $b/a = 0.5$.

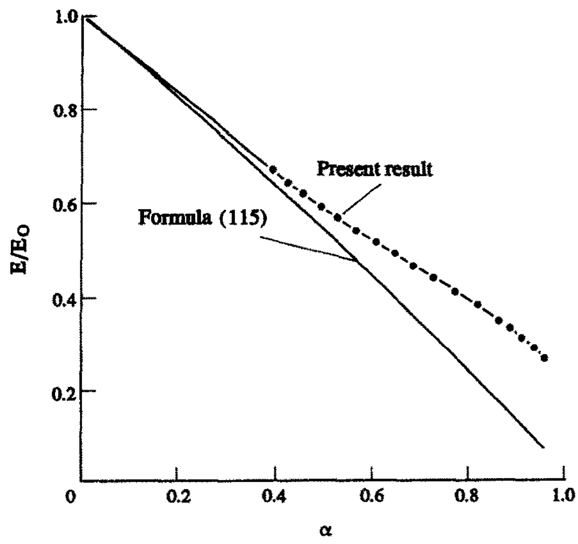

Fig. 13. Comparison of present result ($b/a = 1$) and existing result for the effective Young's modulus.

A comparison of the present results with the results given by Horii and Nemat-Nasser [2] and Suramac and Krajcinovic [5] is shown in Figs 13–15. Their results for the "isotropic damage" can be expressed as:

$$\begin{cases} \dfrac{E}{E_0} = (1-\alpha)\dfrac{1+\nu_0-2\nu_0\alpha}{(1+\nu_0)(1-\nu_0\alpha)^2} \\ \dfrac{\nu}{\nu_0} = \dfrac{(1-\alpha)}{(1-\nu_0\alpha)} \end{cases} \quad \text{for plane strain.} \tag{115}$$

For small α (<0.2), the two results of E/E_0 are coincidental. For large α, the present result of E/E_0 is greater than the result of formula (115). Especially, in the case of $b/a = 0.5$, the result of formula (115) becomes negative when $\alpha > 1$.

As pointed out by Budiansky and O'Connell [1], Horii and Nemat-Nasser [2], and Sumarac and Krajcinovic [5], formula (115) breaks down when $\alpha > 1$. The present results seem to present no such kind of problem.

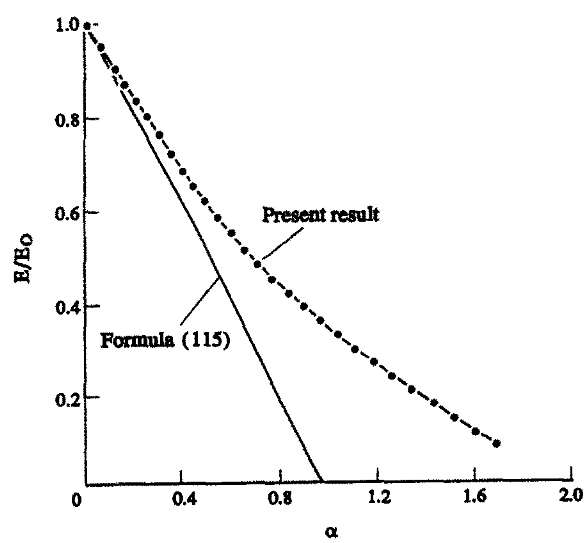

Fig. 14. Comparison of present result ($b/a = 0.5$) and existing result for the effective Young's modulus.

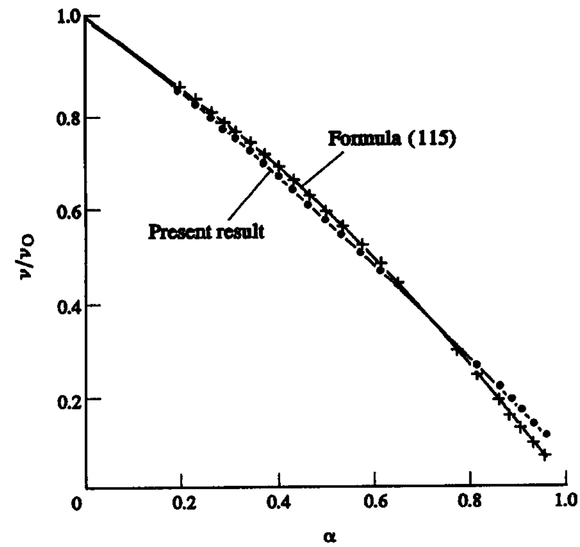

Fig. 15. Comparison of present result ($b/a = 1$) and existing result for the Poisson's ratio.

The present results show that the effective moduli will vanish when the damage parameter ω approaches unity. Figure 15 shows a comparison of the present result ($b/a = 1$) with formula (115) for ν/ν_0. The two results are nearly identical, even for large α.

6. CONCLUSION

A new damage model has been developed in this study, in which the original cracked solid is considered to be an aggregate of the elliptic cells. Each crack is embedded in an elliptic cell. The minor semi-axis and the major semi-axis can be adjusted to give a desired value of crack density parameter and a desired value of damage parameter.

Using the complex potential method, the analytical formulas and the calculation results of the effective moduli and the stress intensity factors for the elliptic cell are obtained for different aspect ratios and different values of damage.

These results may provide a basis for the treatment of more complex and realistic cases of interaction between microcracks surrounded by different materials or different phases.

In Section 4, an analytic closed formula of the concentration factor tensor for an anisotropic inclusion embedded in an isotropic matrix was presented.

The effective elastic moduli of the solids weakened by a doubly periodic array of aligned microcracks or randomly oriented microcracks are obtained.

The present study shows that both the crack density parameter and the damage parameter are important in order to characterize completely the effect of randomly oriented microcracks on the effective elastic moduli of cracked solids.

REFERENCES

[1] B. Budiansky and R. J. O'Connell, Elastic moduli of cracked solid. *Int. J. Solids Structures* **12,** 81 (1976).
[2] H. Horii and S. Nemat-Nasser, Overall moduli of solids with microcracks: load induced anisotropy. *J. Mech. Phys. Solids* **31,** 155 (1983).
[3] A. Hoenig, *Int. J. Solids Structures* **15,** 137 (1979).
[4] T. Grottesmann, Z. Hashin and M. A. Brull, Advances in composite materials. *Proc. ICCM*, Vol. 3, pp. 749–758. Pergamon Press, Oxford (1980).
[5] D. Sumarac and D. Krajcinovic, A self-consistent model for microcrack weakened solids. *Mech. Mater. b*, 39 (1987).
[6] N. Laws and J. R. Brockenbrough, The effect of microcrack systems on the loss of stiffness of brittle solids. *Int. J. Solids Structures* **23,** 1247 (1987).
[7] R. L. Salganik, Mechanics of bodies with many cracks. *Izv. AN SSR, Mekh. Iverdogo Tela* **8,** 149 (1973).
[8] R. M. Christensen and K. H. Lo, Solution for effective shear properties in three phase sphere and cylinder models. *J. Mech. Phys. Solids* **27,** 315 (1979).

[9] A. Litewka, Effective material constants of orthotropically damaged elastic solid. *Arch. Mech.* **37**, 631 (1985).
[10] A. Litewka, On stiffness and strength reduction of solids due to crack development. *Ing. Frac. Mech.* **25**, 637 (1986).
[11] J. Aboudi and Y. Benveniste, The effective moduli of cracked solids in plane deformation. *Engng Fracture Mech.* **26**, 171 (1987).
[12] D. Krajcinovic, Damage mechanics. *Mech. Mater.* **8**, 1 (1989).
[13] L. M. Kachanov, On the creep rupture time. *Izv. AN SSSR, Otd. Tekhn. Nauk* **8**, 26 (1958).
[14] J. Lemaître and J. L. Chaboche, Aspect phénoménalogique de la rupture par endommagement. *J. Mech. Applic.* **2**, 317 (1978).
[15] N. I. Muskhelishvili, *Some Basic Problems of the Mathematical Theory of Elasticity*. P. Noordhoff, The Netherlands (1953).
[16] J. D. Eshelby, *Proc. R. Soc.* **A241**, 376 (1957).

(*Received* 19 *December* 1991)